Love wave suppression without prior structural information

L. F. van Zanen, C. P. A. Wapenaar, G. G. Drijkoningen and J. T. Fokkema

Delft University of Technology, Department of Applied Earth Sciences, PO Box 5028, *Mijnbouwstraat* 120, 2600 *GA Delft, the Netherlands*

SUMMARY

Love waves are one of the major contributors of noise in *SH*-wave reflection data. Suppressing them can be difficult, most importantly because their group velocity is almost equal to the shear wave velocity. By using the Betti-Rayleigh reciprocity theorem for elastic media, modified for *SH* waves only, we derive an integral equation of the second kind for an ideal wavefield that does not contain the Love waves. No structural subsurface model is needed for solving this integral equation. The equation can be solved numerically, for example by a direct matrix inversion. The method is tested on several synthetic data sets, modelled with the finite difference method. We illustrate both the laterally invariant and the laterally varying situation with examples. Finally, we test the sensitivity of the suppression method, and observe that it is relatively the most sensitive to errors in the phase of the source wavelet.

Key words: Love waves, reciprocity, *SH* waves.

1 INTRODUCTION

Two types of elastodynamic waves can propagate through an elastic medium. They are: compressional waves (*P* waves) and shear waves (*S* waves). The shear waves are also divided into two types: waves polarized in a vertical plane (*SV* waves) and horizontally polarized waves (*SH* waves). In many cases, *SH* waves are assumed to be decoupled from the other wave types. Most generally, this is the case when the medium is invariant in the crossline (x_2) direction.

In any elastic medium, the velocity of shear waves is lower than that of *P* waves. In soft soils, the ratio of *P*-wave velocity over *S*-wave velocity can be as high as 10. Therefore, with the same frequency content, a higher resolution and more detail is possible with *SH*-wave reflection experiments, and so, an increased effort has been done to exploit this characteristic. Also, in air- or gas-filled media, *P* waves are often severely scattered, while *S* waves are hardly affected. During recent years, the awareness has grown that *SH*-wave seismic reflection experiments indeed provide an adequate and cost effective method to image the shallow subsurface (Deidda & Balia 2001).

One of the main problems encountered in *SH*-wave reflection seismics is the occurrence of Love waves (Miller *et al.* 2001). Love waves are surface waves (see for example Aki & Richards 1980), and are considered noise in reflection surveys. They can exist in a medium where there is a low (shear wave) velocity layer over further earth layers. Several problems make it difficult to suppress Love waves from *SH*-wave reflection data. Since Love waves propagate along the surface, they attenuate slowly, and account for most of the energy in a seismogram. Also, in shallow surveys, and especially in soft soils, the group velocity of Love waves is almost equal to the horizontal shear wave velocity of reflection events, and therefore Love waves are hard to separate from reflections with filtering techniques based on velocity, such as (f, k)-domain filtering. And we have to deal with the fact that Love waves are dispersive, which means that they have a phase velocity that is frequency dependent.

Past efforts to suppress dispersive events from seismic data include for example Ernst & Herman (1998), who removes scattering effects from surface waves. His approach is to make a model of the subsurface, calculate the response, and subtract that from the data. Or Nguyen *et al.* (1999), who proposes a combination of techniques to remove Rayleigh waves from multi-component data. None of these techniques, however, focuses on Love waves.

In this paper, we present a new method to suppress Love waves in *SH*-wave data. The procedure we follow is similar to that of van Borselen *et al.* (1996), who used acoustic reciprocity to suppress surface related water layer multiples from marine seismic data, with the essential difference that water layer multiples are propagating waves, whereas Love waves occur mainly in the evanescent regime. We use elastic reciprocity. Reciprocity is a mathematical concept by which two different states are related to each other. Here, the two states are (*SH*-) wavefields in an isotropic elastic medium. One state is defined as the actual state, where a (stress-free) surface is present, the other state is the desired state, that differs only from the actual state by the absence of this surface. The final expression is an integral equation, from which the desired wavefield in a medium without a surface can be solved, given the actual measured wavefield in a medium with the Love wave generating surface. This integral equation can be solved numerically with a direct matrix inversion. In the special case that a laterally invariant

medium can be assumed, the equation can be transformed to the horizontal slowness domain, where the kernel of the integral equation becomes diagonal, and hence a very efficient suppression procedure can be derived.

Both the laterally invariant and the laterally varying situation will be discussed and illustrated with examples. We also examine the sensitivity of the method to certain errors. Two distinctions are made for these errors: errors in the input parameters, and errors in the data.

2 THEORY

This section derives the Betti-Rayleigh reciprocity theorem, which will be applied to the *SH*-wave case, i.e. by using a crossline seismic source and crossline receivers. By defining the two proper states, we derive an algorithm for suppressing Love waves from *SH*-wave data, by means of an integral equation of the second kind.

2.1 Basic elastic equations for *SH* waves

In this paper, we use a 2-D Cartesian coordinate system $x = \{x_1, x_3\}$, in which the x_3 axis is pointing downward. The Einstein summation convention for repeated indices is employed, i.e. $a_i b_i$ stands for $a_1 b_1 + a_3 b_3$. The symbol ∂_i will be used as a short-hand notation for the partial derivative with respect to the x_i coordinate.

The wavefield in an elastic medium is described by the elasto-dynamic equations. In the space-Laplace domain (defined in Appendix A), and for *SH* waves in isotropic media these equations read:

$$\partial_j \hat{\tau}_{2,j}(x, s) - s\rho(x)\hat{v}_2(x, s) = -\hat{f}_2(x, s), \tag{1}$$

$$\partial_j \hat{v}_2(x, s) - \frac{s}{\mu(x)}\hat{\tau}_{2,j}(x, s) = 0, \tag{2}$$

in which

$s =$ Laplace parameter,
$\hat{\tau}_{2,j}(x, s) =$ crossline component of the elastic stress tensor,
$\hat{v}_2(x, s) =$ crossline component of the particle velocity,
$\rho(x) =$ volume density of mass,
$\mu(x) =$ shear modulus,
$\hat{f}_2(x, s) =$ volume source density of force, pointing in the crossline direction,

These equations are a modification of the elasto-dynamic equations found in De Hoop (1995).

Reciprocity, in general terms, provides a means to relate two states to each other. Here, of course, we take two elastic states. One elastic state is actually a combination of three states: the field state ($\hat{\tau}_{2,j}$ and $\hat{v}_2$), the material state (ρ and μ) and the source state ($\hat{f}_2$). We label the two states *A* and *B*. For quick reference, these states are summarized in Table 1. Now, we consider the following scalar interaction quantity: $\partial_j(\hat{\tau}_{2,j}^A \hat{v}_2^B - \hat{\tau}_{2,j}^B \hat{v}_2^A)$. First, we apply the product rule and substitute eqs (1) and (2). Next, we integrate the result over a closed 2-D plane $\mathbb{V}$ with boundary $\partial\mathbb{V}$ and an outward pointing normal vector n_j. Then, we apply Gauss' theorem and obtain:

$$\oint_{x \in \partial\mathbb{V}} \left(\hat{\tau}_{2,j}^A \hat{v}_2^B - \hat{\tau}_{2,j}^B \hat{v}_2^A\right) n_j dx = \int_{x \in \mathbb{V}} \left[s\left(\frac{1}{\mu^B} - \frac{1}{\mu^A}\right)\hat{\tau}_{2,j}^A \hat{\tau}_{2,j}^B - s(\rho^B - \rho^A)\hat{v}_2^A \hat{v}_2^B\right] d^2 x + \int_{x \in \mathbb{V}} \left[\hat{f}_2^B \hat{v}_2^A - \hat{f}_2^A \hat{v}_2^B\right] d^2 x. \tag{3}$$

Eq. (3) is the global form of the Betti-Rayleigh reciprocity theorem, modified for the special case of decoupled *SH* waves.

2.2 Description of the reciprocity states

In order to arrive at the algorithm to suppress Love waves in *SH*-wave data, the two states to be compared are a state with a stress-free surface, as is the case in the field, and a state without a surface, and hence no surface effects (like Love waves). Fig. 1 shows a graphical representation of these two states, that will be discussed below. From now on, quantities related to state *A* will have the superscript *surf*, and quantities related to state *B* will have the superscript *nosurf*.

Table 1. States in the *SH*-wave reciprocity theorem.

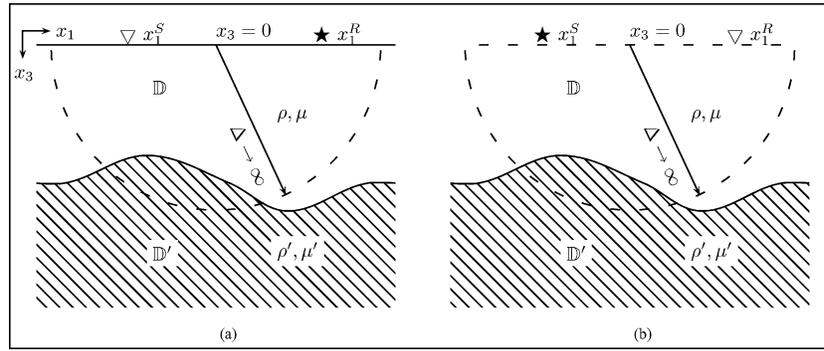|	State *A*	State *B*
Field state	$\{\hat{\tau}_{2,j}^A, \hat{v}_2^A\}(x, s)$	$\{\hat{\tau}_{2,j}^B, \hat{v}_2^B\}(x, s)$
Material state	$\{\rho^A, \mu^A\}(x)$	$\{\rho^B, \mu^B\}(x)$
Source state	$\hat{f}_2^A(x, s)$	$\hat{f}_2^B(x, s)$
	Domain $\mathbb{V}$	

Figure 1. The two states for the reciprocity theorem, with $\mathbb{V} = \mathbb{D} \cup \mathbb{D}'$. (a) State *A*, with stress-free surface, (b) State *B*, without surface. The dashed line is the path of integration, which extends to infinity. $\star$ denotes a source, ∇ denotes a receiver.

2.2.1 The state with a stress-free surface

Here we consider the situation as shown in Fig. 1(a). The domain of integration for eq. (3) is the lower halfspace $\mathbb{V} = \mathbb{D} \cup \mathbb{D}' = \{\boldsymbol{x} \in \mathbb{R}^2 | -\infty < x_1 < \infty, 0 \leq x_3 < \infty\}$. This halfspace consists of a thin homogeneous and isotropic layer $\mathbb{D}$ with an arbitrary shaped lower boundary, and arbitrary inhomogeneous earth layers in domain $\mathbb{D}'$. In this situation, there is a stress-free surface, $\hat{\tau}_{2,3}^{\text{surf}} = 0$ at $x_3 = 0$, which is the cause of surface effects like Love waves. The sources and receivers are situated on this surface. The source is defined as a boundary condition in the stress field. This means that the surface is stress-free, except at a certain point $x_1 = x_1^R$. Hence, the stress is given by: $\hat{\tau}_{2,3}^{\text{surf}}(x_1, x_3 = 0, s) = -\hat{t}_2^{\text{surf}}(s)\delta(x_1 - x_1^R)$, where $\hat{t}_2^{\text{surf}}$ is defined as the traction on the surface in the x_2 direction, and the minus stems from the fact that the normal at the stress-free surface points outward of domain $\mathbb{V}$, i.e. in the negative x_3-direction. The resulting wavefield quantities are denoted for example as: $\hat{v}_2^{\text{surf}}(\boldsymbol{x}|\boldsymbol{x}^R, s)$, which means as much as the cross-component of the particle velocity measured at a position $\boldsymbol{x}$, caused by a source at a position $\boldsymbol{x}^R$.

2.2.2 The state without a surface

In this situation (shown in Fig. 1b), the domain of integration is again the lower halfspace. However, in this state, the upper halfspace is substituted by a medium that bears the same properties as domain $\mathbb{D}$. This means that the plane $x_3 = 0$ is just a reference depth level in a homogeneous halfspace. It is obvious that no surface effects can take place in this configuration. A volume source density of force is defined at $x_1 = x_1^S$: $\hat{f}_2(x_1, x_3, s) = \hat{f}_2^{\text{nosurf}}(s)\delta(x_1 - x_1^S)\delta(x_3)$. The receivers are also situated on the plane $x_3 = 0$. The resulting wavefield quantities are denoted for example as: $\hat{v}_2^{\text{nosurf}}(\boldsymbol{x}|\boldsymbol{x}^S, s)$, which means as much as the crossline component of the particle velocity measured at a point $\boldsymbol{x}$, due to a source at a point $\boldsymbol{x}^S$.

The states for the domain of integration are summarized in Table 2.

2.3 Derivation of the suppression equation

Now, we substitute the states summarized in Table 2 into eq. (3). The path of integration $\partial\mathbb{V}$ is defined as the surface $x_3 = 0$, which is closed by a semi-circle that extends to infinity in the lower halfspace. We apply physical reciprocity (i.e. we switch source and receiver positions) for $\hat{v}_2^{\text{surf}}$, and obtain the following equation:

$$\int_{x_1 \in \mathbb{R}} \hat{\tau}_{2,3}^{\text{nosurf}}\left(x_1, 0 \mid x_1^S, 0, s\right) \hat{v}_2^{\text{surf}}\left(x_1^R, 0 \mid x_1, 0, s\right) dx_1 = \frac{1}{2}\hat{f}_2^{\text{nosurf}}(s)\hat{v}_2^{\text{surf}}\left(x_1^R, 0 \mid x_1^S, 0, s\right) - \hat{t}_2^{\text{surf}}(s)\hat{v}_2^{\text{nosurf}}\left(x_1^R, 0 \mid x_1^S, 0, s\right). \tag{4}$$

The first term on the right hand side of eq. (3) drops, because there is no difference in material parameters for the domain of integration. Since the normal is pointing outward of the domain of integration (upward in this case), the left-hand side of eq. (4) includes an extra minus sign

Table 2. States for the reciprocity theorem, used for the suppression of Love waves. $\boldsymbol{x}^S$ and $\boldsymbol{x}^R$ are located on the surface $x_3 = 0$.

	State *A* (surface state)	State *B* (no-surface state)
Field state	$\{\hat{\tau}_{2,j}^{\text{surf}}, \hat{v}_2^{\text{surf}}\}(\boldsymbol{x}|\boldsymbol{x}^R, s)$	$\{\hat{\tau}_{2,j}^{\text{nosurf}}, \hat{v}_2^{\text{nosurf}}\}(\boldsymbol{x}|\boldsymbol{x}^S, s)$
Material state	$\{\rho, \mu\}$in$\mathbb{D}$	$\{\rho, \mu\}$in$\mathbb{D}$
	$\{\rho', \mu'\}$in$\mathbb{D}'$	$\{\rho', \mu'\}$in$\mathbb{D}'$
Source state	0	$\hat{f}_2^{\text{nosurf}}(s)\,\delta(x_1 - x_1^S)\,\delta(x_3)$
Surface state	Stress-free except at $x_1 = x_1^R$: $\hat{\tau}_{2,3}^{\text{surf}} = -\hat{t}_2^{\text{surf}}(s)$ $\times \delta(x_1 - x_1^R)$	Continuous stress and velocity
	Domain $\mathbb{V} = \mathbb{D} \cup \mathbb{D}'$ (see Fig. 1)	

(which compensates the original minus sign in $-\hat{\tau}_{2,j}^{B}\hat{v}_{2}^{A}$). The factor $\frac{1}{2}$ on the right-hand side is the result of integrating over a delta function located exactly on the boundary of the domain of integration: the surface $x_3 = 0$. The integral along the semi-circle at infinity in eq. (4) yields zero ($\mathcal{O}(\Delta^{-1})$ as $\Delta \to \infty$), due to causality (Fokkema & van den Berg 1993).

We take equal source functions:

$$\hat{f}_{2}^{\text{nosurf}}(s) = \hat{t}_{2}^{\text{surf}}(s) = \hat{f}_{2}(s), \tag{5}$$

and apply Parseval's theorem to eq. (4):

$$\frac{1}{2\pi}\int_{s\alpha_1 \in \mathbb{R}} \tilde{\tau}_{2,3}^{\text{nosurf}}\left(js\alpha_1, 0 \mid x_1^S, 0, s\right) \bar{v}_2^{\text{surf}}\left(x_1^R, 0 \mid js\alpha_1, 0, s\right) ds\alpha_1 = \frac{1}{2}\hat{f}_2(s)\hat{v}_2^{\text{surf}}\left(x_1^R, 0 \mid x_1^S, 0, s\right) - \hat{f}_2(s)\hat{v}_2^{\text{nosurf}}\left(x_1^R, 0 \mid x_1^S, 0, s\right). \tag{6}$$

Notice that we used two different definitions of the horizontal Fourier transform, one for the receiver coordinates (denoted by the tilde $\tilde{\ }$), and one for the source coordinates (denoted by the bar $\bar{\ }$), as explained in Appendix A.

When $\hat{v}_2^{\text{surf}}$ is the measured data, $\hat{v}_2^{\text{nosurf}}$ is to be determined and the source wavelet $\hat{f}_2$ is known, then the only other unknown term in eq. (4) is the stress component $\tilde{\tau}_{2,3}^{\text{nosurf}}$. This term can be written in terms of velocity with the help of eq. (2):

$$\hat{\tau}_{2,3}^{\text{nosurf}} = \frac{\mu}{s}\partial_3\hat{v}_2^{\text{nosurf}}. \tag{7}$$

This operation can be done conveniently in the horizontal slowness domain (defined in Appendix A). There, the differentiation with respect to the x_3 component becomes a multiplication with either $+s\gamma_s$ or $-s\gamma_s$, depending whether the field is an up-going or a down-going field, respectively. γ_s is defined as $\sqrt{\frac{1}{c_s^2} + \alpha_1^2}$, where c_s is defined as the shear-wave velocity of the top layer, and α_1 as the angular slowness. To determine whether the field is up-going or down-going, it is split into an incident and a reflected field:

$$\tilde{v}_2^{\text{nosurf}} = \tilde{v}_2^{\text{inc}} + \tilde{v}_2^{\text{ref}}. \tag{8}$$

The vertical derivative of the incident wavefield $\tilde{v}_2^{\text{inc}}$ is zero, because the sources and receivers are at the same level (the surface $x_3 = 0$), making this wavefield neither up-going nor down-going (see also Appendix B, eq. B5). The reflected wavefield $\hat{v}_2^{\text{ref}}$ is clearly up-going. We find for eq. (7):

$$\tilde{\tau}_{2,3}^{\text{nosurf}} = \mathcal{F}_R\left\{\frac{\mu}{s}\partial_3\hat{v}_2^{\text{nosurf}}\right\} = \mathcal{F}_R\left\{\frac{\mu}{s}\partial_3\hat{v}_2^{\text{ref}}\right\} = \mu\gamma_s\left(\tilde{v}_2^{\text{nosurf}} - \tilde{v}_2^{\text{inc}}\right), \tag{9}$$

where the tilde $(\tilde{\ })$ denotes that the representation is in the horizontal slowness domain, and $\mathcal{F}_R$ denotes the Fourier transformation as defined in Appendix A. The incident wavefield in the *SH*-wave case can be written in the horizontal slowness domain as:

$$\tilde{v}_2^{\text{inc}}\left(js\alpha_1, 0 \mid x_1^S, 0, s\right) = \frac{\hat{f}_2(s)}{2\mu\gamma_s}e^{js\alpha_1 x_1^S}. \tag{10}$$

The derivation of this equation, which is not completely trivial, is given in Appendix B. With this, the goal of writing the stress-field in terms of velocity is complete.

Finally, we substitute eqs (9) and (10) into eq. (6) and obtain:

$$\frac{1}{2\pi}\int_{s\alpha_1 \in \mathbb{R}} \frac{\mu\gamma_s}{\hat{f}_2(s)}\bar{v}_2^{\text{surf}}\left(x_1^R, 0 \middle| js\alpha_1, 0, s\right)\tilde{v}_2^{\text{nosurf}}\left(js\alpha_1, 0\middle| x_1^S, 0, s\right) ds\alpha_1 = \hat{v}_2^{\text{surf}}\left(x_1^R, 0\middle| x_1^S, 0, s\right) - \hat{v}_2^{\text{nosurf}}\left(x_1^R, 0\middle| x_1^S, 0, s\right). \tag{11}$$

This is an integral equation of the second kind, meaning that the unknown term ($\hat{v}_2^{\text{nosurf}}$) is both inside and outside the integral. The quantities to be known are: the measured data with the surface effects ($\hat{v}_2^{\text{surf}}$), the source wavelet ($\hat{f}_2$), and the material parameters of the top layer ($\mu\ \gamma_s$). No model is needed for the structure of the top layer or further layers. The wavelet is either assumed to be known (or measured) or estimated from the data. The material parameters are also assumed to be known (for example by taking samples of the soil).

2.4 Horizontally layered media

When we take a special case of horizontally layered configurations, the data is dependent on the distance between the source and receivers only (at least in our configuration, where both are situated on the surface). We can write:

$$\hat{v}_2^{\text{surf}}\left(x_1^R, 0\middle| x_1^S, 0, s\right) = \hat{v}_2^{\text{surf}}\left(x_1^R - x_1^S, 0, s\right). \tag{12}$$

Applying a Fourier transformation on the receiver coordinates to the horizontal slowness domain (as defined in Appendix A), we get:

$$\tilde{v}_2^{\text{surf}}\left(js\alpha_1^R, 0\middle| x_1^S, 0, s\right) = \int_{x_1^R \in \mathbb{R}} \hat{v}_2^{\text{surf}}\left(x_1^R - x_1^S, 0, s\right) e^{js\alpha_1^R x_1^R} dx_1^R$$
$$= \tilde{v}_2^{\text{surf}}\left(js\alpha_1^R, 0, s\right) e^{js\alpha_1^R x_1^S}. \tag{13}$$

After another Fourier transformation to the source coordinates, we obtain:

$$\tilde{\bar{v}}_2^{\text{surf}}\left(js\alpha_1^R, 0\middle| js\alpha_1^S, 0, s\right) = 2\pi\tilde{v}_2^{\text{surf}}\left(js\alpha_1^R, 0, s\right)\delta\left(s\alpha_1^R - s\alpha_1^S\right). \tag{14}$$
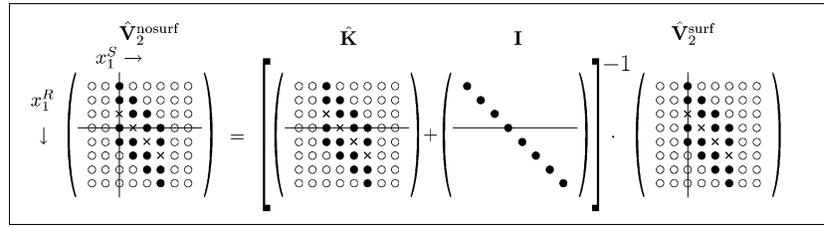
Figure 2. Procedure for solving a set of linear equations in the space-Laplace domain to obtain one Love-wave-free trace (denoted by the crossing of the lines on the left-hand side). A circle represents a padded zero, a disc a receiver and a cross a source position. The lines on the right hand side indicate the source and receiver positions involved in the numerical procedure.

The same arguments are used for $\hat{v}_2^{\text{nosurf}}$. When we apply a double Fourier transformation to eq. (11), with respect to both x_1^R and x_1^S, and substitute eq. (14), we obtain a simple analytical expression:

$$\tilde{v}_2^{\text{nosurf}} = \frac{\tilde{v}_2^{\text{surf}}}{1 + \frac{\tilde{v}_2^{\text{surf}}}{2\tilde{v}_2^{\text{inc}}}}, \tag{15}$$

where we also used eq. (10).

2.5 Numerical implementation for laterally varying media

When the data are discrete, eq. (11) can be written as a matrix equation. The discrete counterparts of $\hat{v}_2^{\text{surf}}(x_1^R|x_1^S, s)$ and $\hat{v}_2^{\text{nosurf}}(x_1^R|x_1^S, s)$ (where we omitted the $x_3^R = x_3^S = 0$ dependence) are denoted with bold, uppercase $\hat{\mathbf{V}}_2^{\text{surf}}$ and $\hat{\mathbf{V}}_2^{\text{nosurf}}$, respectively. These are (2-D) matrices, where the organization is, from fastest to slowest dimension: x_1^R and x_1^S, and where s is a parameter.

Now, we examine the operation $\mu\gamma_s$ in eq. (11) operating on $\tilde{v}_2^{\text{nosurf}}$. It is the result of writing the no-surface stress field in terms of velocity. But in the horizontal slowness domain we notice that this operation can alternatively be applied to $\tilde{v}_2^{\text{surf}}$, but with the Fourier transform applied to the source positions, instead of the receiver positions. The equation is transformed back to the space-Laplace domain with the help of Parseval's theorem:

$$\mathcal{F}_S^{-1}\left\{\frac{\mu\gamma_s}{\hat{f}_2(s)}\mathcal{F}_S\left\{\hat{\mathbf{V}}_2^{\text{surf}}\right\}\right\} \cdot \hat{\mathbf{V}}_2^{\text{nosurf}}\Delta x_1 = \hat{\mathbf{V}}_2^{\text{surf}} - \hat{\mathbf{V}}_2^{\text{nosurf}}. \tag{16}$$

This is rewritten as:

$$\hat{\mathbf{V}}_2^{\text{nosurf}} = \left[\mathcal{F}_S^{-1}\left\{\frac{\mu\gamma_s}{\hat{f}_2(s)}\mathcal{F}_S\left\{\hat{\mathbf{V}}_2^{\text{surf}}\right\}\right\}\Delta x_1 + \mathbf{I}\right]^{-1} \cdot \hat{\mathbf{V}}_2^{\text{surf}}. \tag{17}$$

In this equation, $\mathbf{I}$ is the unity matrix. This equation can be solved with a direct matrix inversion. Fig. 2 shows the organization of the matrices when the data is *split spread* (when there are as many receivers with negative offset as with positive offset). In this figure, the term with the Fourier transforms has been symbolized by $\hat{\mathbf{K}}$ (for *kernel*). It is the discretized form of the kernel of the integral equation, eq. (11). This kernel consists of the data with Love waves ($\hat{\mathbf{V}}_2^{\text{surf}}$), where we applied a deconvolution to eliminate the source signature, and a vertical impedance correction (notice that $\mu\gamma_s$ has the same unit as impedance, and that it comes from a vertical derivative of the stress-field).

3 NUMERICAL TESTS AND RESULTS

The Love wave suppression scheme is tested on several synthetic data sets. The data sets are created using finite difference modelling as developed by Falk (1998). While the structural model differs in the data sets, the material parameters were the same for all. First, there is a thin, Love wave generating layer with a shear wave velocity of $c_s = 200$ m s^{-1}, then a thicker layer with a shear wave velocity of $c_s = 300$ m s^{-1}, and finally the lower halfspace, which has a shear wave velocity of $c_s = 350$ m s^{-1}. The mass density is the same for all layers: $\rho = 2000$ kg m^{-3}. Source and receiver spacing is 0.8 m. The sampling interval is 0.001 s. As a source function, we use a Ricker-wavelet, with a peak frequency of 33.333 Hz, and which is shifted in time to make it (almost) causal. The data are tapered to reduce edge effects that are caused by spatial windowing, and only the non-tapered parts are shown. For the implementation of eqs (17) and (15), we use a complex Laplace parameter: $s = \varepsilon + j\omega$, where ω is the angular frequency, and an independent value of $\varepsilon = 4$ is chosen.

3.1 A horizontally layered medium

For the first example we use a horizontally layered medium. The first layer has a thickness of 1.2 m, the second layer has a thickness of 22.0 m. Fig. 3(a) shows a common source gather of this configuration. The most dominant events in this figure are the Love waves. They are clearly dispersive. The reflection from the deeper layer can be seen as a hyperbolic event at small offsets. For larger offsets, the Love waves obscure the reflection.
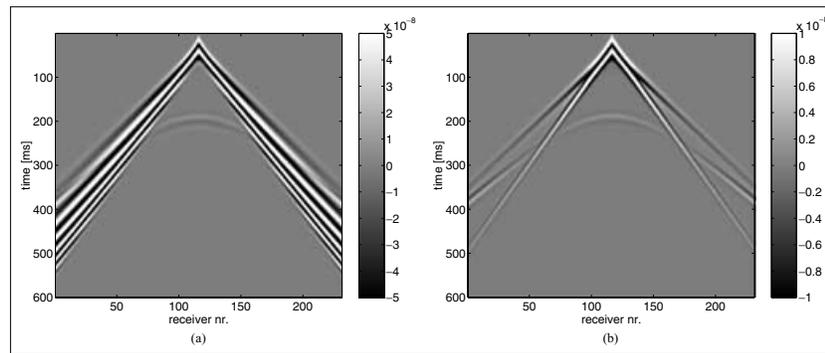
Figure 3. (a) Common source gather including Love waves, in a horizontally layered medium, (b) after application of suppression procedure (eq. 15).

Fig. 3(b) shows the source gather after the application of eq. (15). The Love waves have been completely suppressed. All that remains in this gather, are the direct *SH* wave, which interferes with the reflection of the first layer, and the refraction of the first layer. More of the reflection of the deeper layer is visible, and its amplitude ratio with respect to the other events in this gather is higher when compared to Fig. 3(a).

3.2 A medium with a complex interface

As a second example, we model the response of a medium in which the interface of the shallow layer makes several jumps, thus varying the depth of the Love wave generating layer between 0.4 m and 2.8 m. Fig. 4(a) shows a graphical representation of this model. 251 common source gathers were modelled with 241 traces each. Fig. 4(b) shows a common source gather in the middle of the data set. In addition to the Love waves, which are again dominant, we observe other noise in the form of scattered Love waves, as a result of the jumps in the interface.

For the implementation of eq. (17), we used a direct matrix inversion. Fig. 4(c) shows the result of the suppression procedure. Again, the Love waves, including the scattered ones, have been completely suppressed.
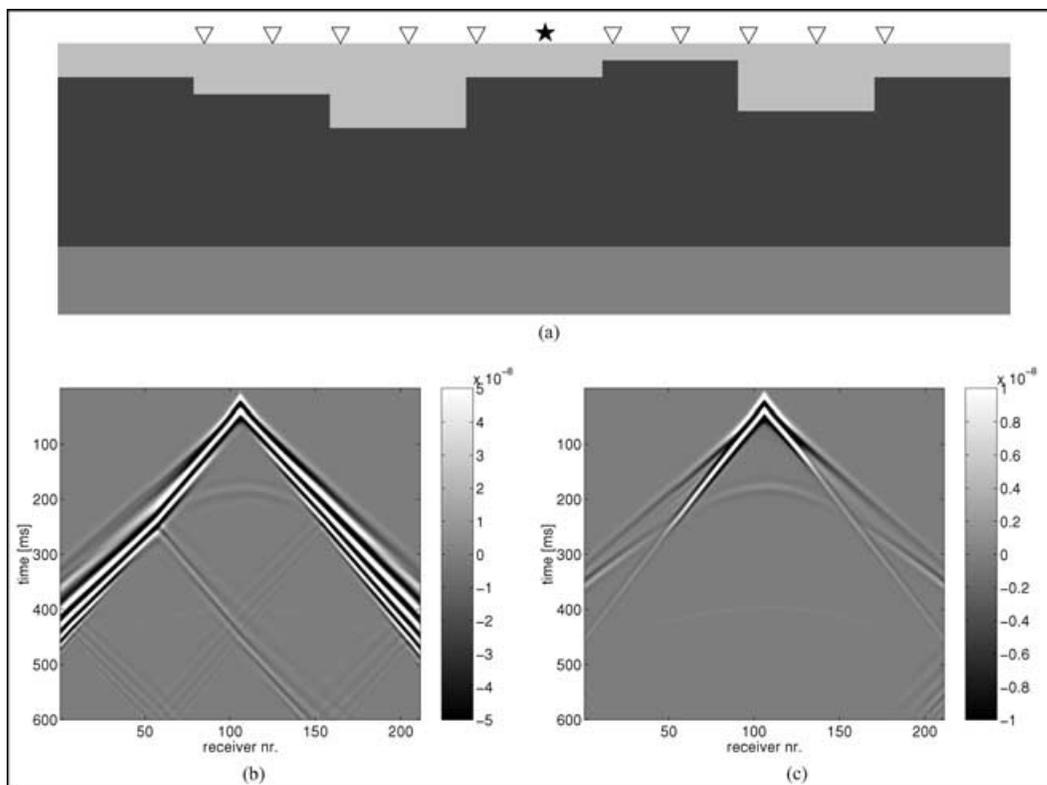

Figure 4. (a) Simplified forward model for the data set, ⋆ denotes the source, ▽ denotes receivers, (b) Common source gather including Love waves, in a medium with a complex interface, (c) after application of suppression procedure (eq. 17).
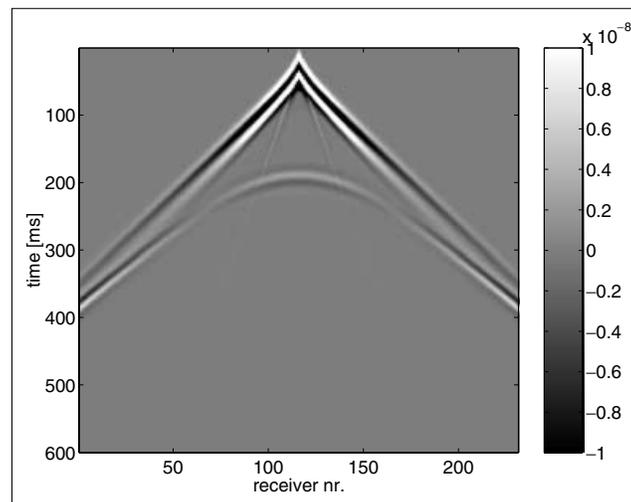
Figure 5. Result of suppression method, when the velocity is underestimated.

3.3 Sensitivity of the method

This section explores the sensitivity of the method. In the previous two sections, it was shown that the method works perfectly on synthetic data. But with synthetic data, the forward model is known exactly. This is of course not the case with field data. Therefore, we test the method for its strengths and weaknesses. This testing can be divided into two parts: taking erroneous input parameters, and taking distorted input data.

The simplest case of the horizontally layered medium was used, so that eq. (15) can be used. The model of the medium is described in Section 3.1.

3.3.1 Sensitivity to errors in the input parameters

The suppression method requires two scalar input parameters. They are: the shear wave velocity c_s and the shear modulus μ of the upper layer. Since the shear modulus can be written as $\mu = \rho c_s^2$, the mass density can also be used. As a typical example, we explore the effect of an erroneous estimation of the velocity on the method.

Fig. 5 shows the result of the suppression method, when the velocity is estimated two times too low, i.e. 100 m s^{-1} instead of 200 m s^{-1}. The Love waves are still suppressed perfectly. The only thing is that the direct wave (which originally had a velocity of 200 m s^{-1}) is replaced by one with a velocity of 100 m s^{-1}, which was to be expected.

Similar results are obtained when the velocity of the top layer was chosen two times too high. Even more interesting is the fact that the mass density of the top layer can be chosen up to ten times too high, and the method still produces good results. It just reduces the total energy in the gather.

3.3.2 Sensitivity to distorted data

In addition to unknown parameters, the data can also be distorted in ways which are not described by the theory. As an example, we examine the effect of anelastic attenuation on the suppression method.

A wave described by the elastic wave theory will continue to propagate through the medium indefinitely. The wave will attenuate spatially, but the total energy of the particle motion in the medium will be preserved. Observations in the field show this idealization to be inaccurate. A wavefield will attenuate through a number of processes, which we will describe as being anelastic. Aki & Richards (1980) give a description of the effects of anelastic attenuation, via a *quality factor Q*. A high value of *Q* means a high 'quality' of the medium, that acts mainly elastic, while a low value means a low 'quality' of the medium, with much attenuation. In the shallow region (the upper 50 m), when the soil is soft and unconsolidated, the quality factor can be as low as 5.

Fig. 6(a) shows the data on which anelastic attenuation is introduced. A quality factor of 10 was used. Fig. 6(b) shows the data after application of the suppression method. The Love waves are still suppressed very well. The method introduces a direct wave which is not attenuated. However, this was also to be expected.

Other distortions of the data that were examined are: the addition of white noise, the removal of a trace from the data, and even (slightly) spatially aliased data. With each of these distortions, the method still produces good results.

3.3.3 Concerning 3-D effects in field data

The method we described assumes 2-D data, or, more precise, data where all sources are line sources that exert their forces in the x_2-direction. The examples we gave in the previous sections were made with a finite difference method, which generated 2-D data. These data show a
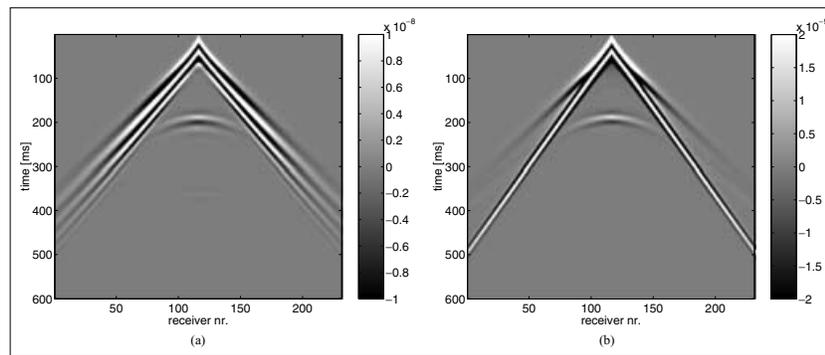
Figure 6. (a) Common source gather with anelastic attenuation introduced in the data, (b) after application of suppression procedure.

cylindric symmetry, with a corresponding amplitude decay proportial to $1/\sqrt{|x|}$ for body waves in the far field. But field data, generated in a 3-D world by (approximately) point sources, show an amplitude decay proportional to $1/|x|$ for body waves (so called spherical divergence). Several methods exist to correct for this discrepancy in amplitude decay (Wapenaar *et al.* 1992). The most common method used is to multiply the field data with offset-independent factors of $\sqrt{j\omega}$ in the frequency domain and $\sqrt{t}$ in the time domain.

This amplitude problem is similar to the anelastic attenuation problem of the previous section. Therefore we also performed the following test on the synthetic data. We transformed these data to (pseudo) 3-D data with the inverse of the procedure described above, and then performed the suppression method on these transformed data. This proved to be no problem for the method. The resulting pictures were very similar to Fig. 3, and therefore we chose not to display them here.

3.3.4 Sensitivity to errors in the source wavelet

As a final example, we test the sensitivity of the method to errors in the source wavelet. As can be seen in eq. (11) or eq. (17), the method performs a deconvolution step, i.e. the data is divided by the source wavelet. This could be a sensitive procedure. We will focus here on the sensitivity to errors in the *phase* of the wavelet, because a deviation in the *amplitude* of the wavelet is equivalent to a deviation in the shear modulus μ (or equivalently, in the mass density ρ). And as we stated in Paragraph 3.3.1, the method is not very sensitive to that.

As explained before, for the forward modelling, we used a shifted version of the Ricker wavelet, which was then almost causal. Next, we applied a phase shift of 60 degrees to this wavelet, and used this resulting wavelet in the suppression procedure. Fig. 7(a) shows these two wavelets.

Fig. 7(b) shows the result of the suppression procedure where the phase-shifted wavelet was used. The Love waves are not completely suppressed anymore, and some noise is added to the data. When the phase shift becomes bigger and bigger, more noise is added faster and faster, and the Love waves are also suppressed much more poorly.

The distortions in the phase of the wavelet are the only example of errors that introduces noise in the data. Therefore, if the source wavelet is unknown, then this implies that it can be estimated from the data with a wavelet estimation procedure based on energy minimization.
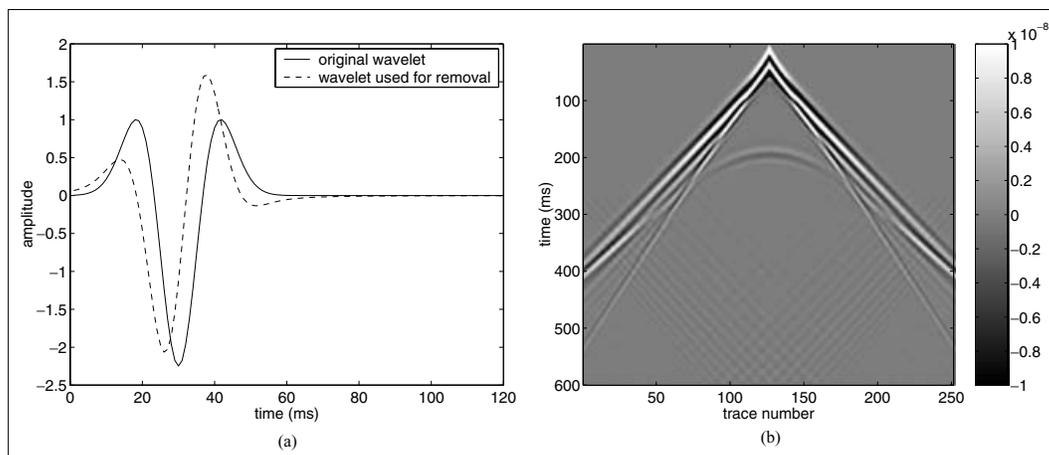

Figure 7. (a) the solid line is the wavelet used in the forward modelling, the dashed line is the wavelet used in the suppression procedure, (b) result of suppression procedure with the (dashed) wavelet of (a).

4 CONCLUSIONS

By using the Betti-Rayleigh reciprocity theorem, we derived a procedure to suppress Love waves in *SH* wave reflection data. No structural subsurface model is needed. The method only needs the material parameters of the top layer, and the source wavelet. When the medium is horizontally layered, the suppression equation becomes a simple explicit scalar expression. Otherwise it is an integral equation of the second kind. This integral equation can be written as a matrix equation, which can be solved numerically by e.g. a direct matrix inversion.

The method has been tested on several synthetic data sets. The first example was a case of a horizontally layered medium. The Love waves in these data were suppressed using the explicit scalar expression. The second example was a case of a medium where the Love wave generating layer made several jumps. In this example, not only the direct Love waves were removed, but also their scattering effects.

Finally we tested the sensitivity of the method to various distortions. The method was not very sensitive to errors in the input parameters. As long as they are chosen within the order of magnitude of the real value, the method will provide good results. The data itself can be distorted, for example by exhibiting anelastic attenuation, and the method will still provide good results. The method is relatively the most sensitive to the phase of the source wavelet. When the phase of the wavelet is shifted by 60 degrees, the results are still reasonably good, but larger shifts in the wavelet will give worse results, and introduce noise into the data.

REFERENCES

Aki, K. & Richards, P.G., 1980. *Quantitative Seismology: Theory and Methods,* W.H. Freeman and Co, San Francisco.

Arfken, G., 1985. *Mathematical methods for physics,* Academic Press, Inc., San Diego.

de Hoop, A.T., 1995. *Handbook of Radiation and Scattering of Waves,* Academic Press, London.

Deidda, G.P. & Balia, R., 2001. An ultrashallow *SH*-wave seismic reflection experiment on a subsurface ground model, *Geophysics,* **66,** 1097–1104.

Ernst, F. & Herman, G.C., 1998. Reduction of near-surface scattering effects in seismic data, *The Leading Edge,* **17,** 759–764.

Falk, J., 1998. Efficient seismic modelling of small-scale inhomogeneities by the finite-difference method, *PhD thesis*, University of Hamburg, Hamburg.

Fokkema, J.T. & van den Berg, P.M., 1993. *Seismic Applications of Acoustic Reciprocity,* Elsevier, Amsterdam.

Miller, R.D., Xia, J., & Park, C.B., 2001. Love waves: A menace to shallow shear wave reflection surveying, in, *71st. Ann. int. mtg., Soc. Expl. Geophys., Expanded Abstracts*, pp. 1377–1380.

Nguyen, M., Glangeaud, F., & Mars, J., 1999. Mixed surface waves elimination, in *61th Annual Mtg., Eur. Ass. of Geosc. & Eng., Expanded Abstracts,* pp. 6–21.

van Borselen, R.G., Fokkema, J.T., & van den Berg, P.M., 1996. Removal of surface-related wave phenomena—the marine case, *Geophysics,* **61,** 202–210.

Wapenaar, C., Verschuur, D., & Hermann, P., 1992. Amplitude preprocessing of single and multicomponent seismic data, *Geophysics,* **57,** 1178–1188.

APPENDIX A: INTEGRAL TRANSFORMS

A1 Laplace transform

The Laplace transformation (Arfken 1985) is defined for a causal function $u(t)$ as:

$$\hat{u}(s) = \int_0^\infty e^{-st} u(t)\, dt. \tag{A1}$$

Here, $\mathrm{Re}(s) > 0$, and the hat (ˆ) denotes that the representation is in the Laplace domain. When we make s completely imaginary ($s = j\omega$, where ω is the angular frequency) we obtain a Fourier transformation to the angular frequency domain. The Laplace transformation is chosen because it is a more stable integral transform.

A2 Transformations to the horizontal slowness domain

In this paper one frequently encounters notations such as: $\hat{u}(x_1^R | x_1^S, s)$. This notation means a field $\hat{u}$, measured at position x_1^R, caused by a source at position x_1^S.

The horizontal Fourier transformation with respect to the receiver coordinates is defined as:

$$\mathcal{F}_R\left\{ \hat{u}\left(x_1^R \mid x_1^S, s\right)\right\} = \tilde{u}\left(js\alpha_1^R \mid x_1^S, s\right) = \int_{x_1^R \in \mathbb{R}} \hat{u}\left(x_1^R \mid x_1^S, s\right) e^{js\alpha_1^R x_1^R}\, dx_1^R, \tag{A2}$$

where α_1^R is defined as the horizontal slowness. Whilst α_1^R may be complex, we choose $s\alpha_1^R$ such that this quantity is real-valued.

For the horizontal Fourier transformation with respect to the source coordinates, we write:

$$\mathcal{F}_S\left\{ \hat{u}\left(x_1^R \mid x_1^S, s\right)\right\} = \bar{u}\left(x_1^R \mid js\alpha_1^S, s\right) = \int_{x_1^S \in \mathbb{R}} \hat{u}\left(x_1^R \mid x_1^S, s\right) e^{-js\alpha_1^S x_1^S}\, dx_1^S. \tag{A3}$$

Notice the different sign in the exponent.

With the two different definitions of the Fourier transform, Parseval's theorem becomes:

$$\int_{x_1 \in \mathbb{R}} \hat{g}\left(x_1^R \mid x_1, s\right) \hat{h}\left(x_1 \mid x_1^S, s\right)\, dx_1 = \frac{1}{2\pi} \int_{s\alpha_1 \in \mathbb{R}} \bar{g}\left(x_1^R \mid js\alpha_1, s\right) \tilde{g}\left(js\alpha_1 \mid x_1^S, s\right)\, ds\alpha_1. \tag{A4}$$

APPENDIX B: THE INCIDENT *SH* WAVEFIELD

We begin by restating eq. (1) and eq. (2):

$$\partial_j \hat{\tau}_{2,j} - s\rho \hat{v}_2 = -\hat{f}_2, \tag{B1}$$

$$\hat{\tau}_{2,j} = \frac{\mu}{s} \partial_j \hat{v}_2. \tag{B2}$$

For the volume density of force, we take a source which exerts its force in the x_2 direction: $\hat{f}_2(\mathbf{x}, s) = \hat{f}_2(s)\delta(x_1 - x_1^S)\delta(x_3 - x_3^S)$. This source generates only *SH* waves. We substitute eq. (B2) into eq. (B1), assume a homogeneous medium and obtain:

$$\frac{\mu}{s} \partial_j \partial_j \hat{v}_2 - s\rho \hat{v}_2 = -\hat{f}_2(s)\delta(x_1 - x_1^S)\delta(x_3 - x_3^S). \tag{B3}$$

With a Fourier transformation to the horizontal slowness domain, this equation becomes:

$$\partial_3^2 \tilde{v}_2 - s^2 \gamma_s^2 \tilde{v}_2 = -\frac{s}{\mu} \hat{f}_2(s) e^{js\alpha_1 x_1^S} \delta(x_3 - x_3^S), \tag{B4}$$

where γ_s is defined as $\sqrt{\frac{1}{c_s^2} + \alpha_1^2}$, and where we have used that $c_s = \sqrt{\mu/\rho}$ The solution to this second order differential equation is well known (Fokkema & van den Berg 1993):

$$\tilde{v}_2 \left(js\alpha_1, x_3 \mid x_1^S, x_3^S, s \right) = \frac{\hat{f}_2(s)}{2\mu\gamma_s} e^{js\alpha_1 x_1^S - s\gamma_s |x_3 - x_3^S|}. \tag{B5}$$

From this equation, it is immediately obvious that a differentiation to the x_3 coordinate gives a multiplication with $-s\gamma_s$ when the wavefield is down-going, and $+s\gamma_s$ when it is up-going.